Hindawi Publishing Corporation
Shock and Vibration
Volume 2014, Article ID 565181, 10 pages
http://dx.doi.org/10.1155/2014/565181

Research Article

Mathematical Modeling of a Transient Vibration Control Strategy Using a Switchable Mass Stiffness Compound System

Diego Francisco Ledezma-Ramirez,[1] Neil Ferguson,[2] and Adriana Salas Zamarripa[1]

[1] *Universidad Autónoma de Nuevo León, Facultad de Ingeniería Mecánica y Eléctrica. Avenida Universidad s/n, 66451 San Nicolás de los Garza, NL, Mexico*
[2] *Institute of Sound and Vibration Research, University of Southampton, Southampton SO17 1BJ, UK*

Correspondence should be addressed to Diego Francisco Ledezma-Ramirez; diego.ledezmard@uanl.edu.mx

Received 1 November 2013; Accepted 10 March 2014; Published 31 March 2014

Academic Editor: Jeong-Hoi Koo

A theoretical control strategy for residual vibration control resulting from a shock pulse is studied. The semiactive control strategy is applied in a piecewise linear compound model and involves an on-off logic to connect and disconnect a secondary mass stiffness system from the primary isolation device, with the aim of providing high energy dissipation for lightly damped systems. The compound model is characterized by an energy dissipation mechanism due to the inelastic collision between the two masses and then viscous damping is introduced and its effects are analyzed. The objective of the simulations is to evaluate the transient vibration response in comparison to the results for a passive viscously damped single degree-of-freedom system considered as the benchmark or reference case. Similarly the decay in the compound system is associated with an equivalent decay rate or logarithmic decrement for direct comparison. It is found how the compound system provides improved isolation compared to the passive system, and the damping mechanisms are explained.

1. Introduction

Mechanical shock is a common problem characterized by a suddenly applied excitation in a short period of time. Usually it involves very large forces and displacements which could lead to damage to sensitive equipment, human discomfort, and other effects [1]. Thus the effective isolation of shock generated vibration is a very important matter in engineering. Shock isolation is normally achieved through energy storage by elastic foundations but optimum isolation is compromised due to the high energy levels requiring large deformations of the isolator where normally space is a constraint. Additionally the isolation system must be able to dissipate the stored energy quickly once the shock has finished in order to minimize residual vibrations.

The classical approach to shock isolation is based on a single degree-of-freedom system with linear stiffness and viscous damping elements. Many shock scenarios can be analyzed considering this method to select proper isolators. Most of the literature related to shock isolation dates from 1950 to 1960 when authors like Ayre [2], Snowdon [3], and Eshleman and Rao [4] studied this phenomenon and settled the fundamental theory of shock analysis and isolation. However, linear passive elements are limited. For instance, there is the compromise aforementioned between isolation performance and space limitations. In order to improve shock isolation, the use of variable or switchable rate elements has been considered. Optimal shock isolation has been considered by Balandin et al. [5] where a performance index and a design constraint are used to design an isolator, obtaining time optimal functions for the isolator. The concept of an early warning or preacting isolator has also been studied, showing a substantial performance increase over typical isolators [6]. Waters et al. devised a dual rate damping strategy where the damping was reduced to a lower value whilst a shock input is applied [7]. Ledezma et al. applied several well-known variable damping skyhook strategies to a single degree-of-freedom system subjected to pulse excitations [8].

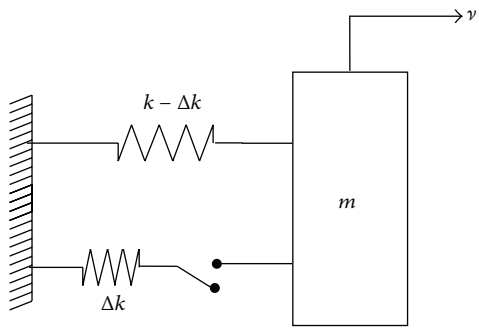

Figure 1: Single degree-of-freedom system with on-off switchable stiffness.

Ledezma has also recently presented a switchable stiffness strategy in two stages, namely, the control during a shock and the later stiffness switching to reduce residual vibrations. This study demonstrated theoretically and experimentally that reducing the stiffness for the duration of a shock reduces the peak response of the system [9, 10].

The approach presented in this work follows a semiactive theoretical strategy based on a piecewise linear compound model, comprised of a main system, that is, the mass to be isolated supported by elastic elements, and a secondary mass spring model which can be attached to or disconnected from the main system. By the use of such model it is expected to gain improved shock isolation and quick dissipation of residual vibrations. The hypothesis is that by transferring part of the energy of the main system to the secondary system it can be dissipated faster as the secondary system oscillates at a higher frequency once it is disconnected. The analysis presented here studies the energy dissipation mechanism for residual vibrations only, when the compound system is subjected to an initial velocity, that is, a very short pulse, focusing on the times when the secondary system is disconnected, and then connected by an inelastic impact to the main mass, thus dissipating energy. It is found how energy dissipation can be maximised if proper values of the mass and stiffness ratios are chosen.

2. A Semiactive Control Strategy for Residual Vibration Control

A control strategy presented by Onoda et al. [11] involves the semiactive switching of the stiffness during the residual period, that is, when a certain shock pulse ends and the system undergoes free vibration. The objective is to quickly dissipate the energy stored by the elastic element during the shock without adding an external damping mechanism. Considering a single degree-of-freedom system with a switchable stiffness element Δk subjected to an initial velocity impulse as given in Figure 1, the control law is given by

$$k_{\text{effective}} = \begin{Bmatrix} k & v\dot{v} \geq 0 \\ k - \Delta k & v\dot{v} < 0 \end{Bmatrix}, \quad (1)$$

where $\dot{v}$ is the velocity of the mass.

The residual control strategy has to ensure that the amplitude of vibration decreases every cycle. The stiffness should be maximum and equal to k when the product $v\dot{v}$ is positive and minimum and equal to $k - \Delta k$ when $v\dot{v}$ is negative. When the displacement response satisfies the condition $v\dot{v} \geq 0$ the displacement v and the velocity $\dot{v}$ have the same sign. As a result the secondary spring, Δk, is disconnected when the absolute value of the *displacement* of the mass is a *maximum*. It is connected again when the absolute value of the *velocity* is a *maximum*, when the system passes through its equilibrium position. The phase plane plot presented in Figure 2(a) shows how the switching occurs effectively dissipating the energy at every stiffness reduction point. Figure 2(b) depicts a time history corresponding to this example.

A comprehensive study of this strategy is also presented in [9], concluding that a greater stiffness reduction leads to greater rate of reduction of the residual vibrations. The study presented by Ledezma-Ramirez et al. [9, 10] assumed that the model involved massless elastic elements. The incorporation of mass with the secondary elastic element represents a further step in the modeling of the system.

3. Compound Model for Residual Vibration Suppression

The concept introduced here considers a secondary spring-mass system that is allowed to connect and disconnect from a main system following a switching logic as depicted in Figure 3. Figure 3(a) shows the rigidly connected model with the response quantity $v(t)$ whilst Figure 3(b) shows the disconnected systems with response quantities $v_1(t)$ and $v_2(t)$ for the primary and secondary systems, respectively. Although the system might look like a two degree of freedom model, the secondary and main systems are not coupled thus they represent two separate SDOF systems when disconnected.

The secondary spring-mass system is allowed to connect and disconnect from the main mass following the control law as given by (1). Considering that the secondary mass-spring system will oscillate independently during the off part of the control law (low stiffness stage), it is important to ensure that the secondary mass is exactly at the static equilibrium position at the moment of stiffness recovery, when the secondary stiffness Δk reconnects to the primary mass. If this is achieved, both the main and the secondary system will coincide at the correct time as given by the control law. This also requires that the primary and secondary systems oscillate in such a way that they do not collide during the time they are disconnected.

One of the principal characteristics of the simple model considered in previous studies [9, 10] is the immediate energy loss at the time at which the secondary stiffness is disconnected, which are the stiffness reduction points shown in Figures 2(a) and 2(b). However, the new approach shown in Figure 3 considers no energy loss during the disconnection. The total energy is the sum of the energy in the main and the secondary system, the latter has a certain amount of potential

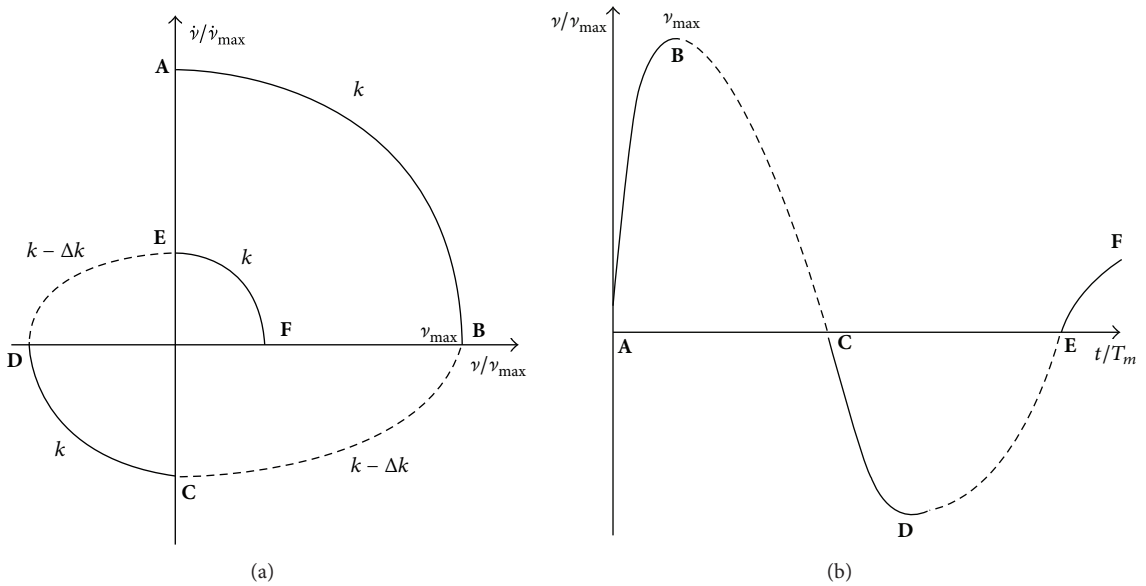

FIGURE 2: Free vibration of the on-off switchable system illustrating the effects of the stiffness change (— high stiffness; - - - low stiffness). (a) Phase plane plot, (b) time history of the displacement response. Response quantities have been normalized to their respective maximum values, and time is normalized considering the mean period $T_m = (T_{on} + T_{off})/2$.

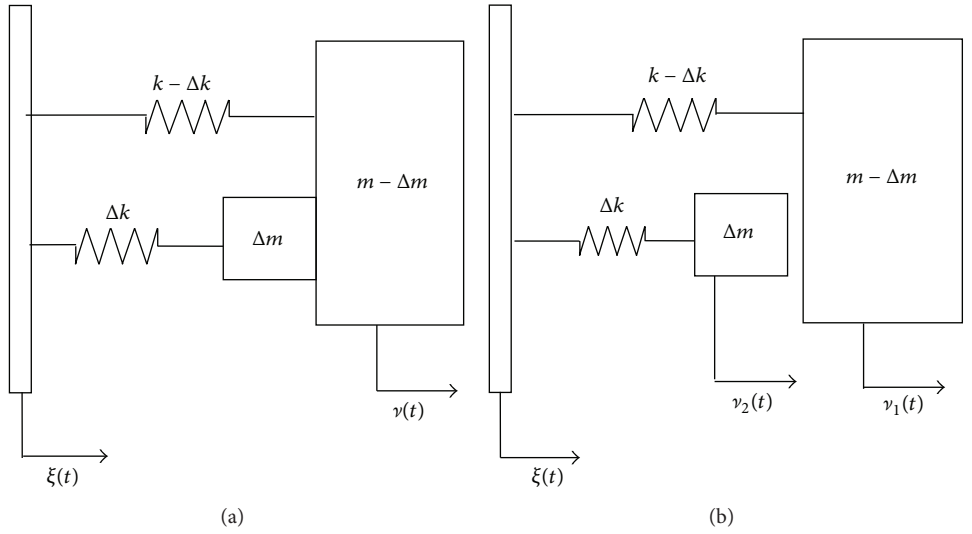

FIGURE 3: Compound model comprising two single degree-of-freedom models that can oscillate together (a) or independently (b).

energy when it is disconnected, and no external or internal form of damping is considered.

For this model the energy dissipation mechanism is attributed solely to the subsequent connection and the impact between the main mass $m - \Delta m$ and the secondary mass Δm. When the impacting masses stick together after the impact then the collision is said to be perfectly inelastic. In this case, the ratio between the velocities of separation and approach of the two masses involved in the impact, also called the coefficient of restitution [12], is zero. The masses will then have the same velocity immediately after the impact, which is according to the conservation of momentum principle given by

$$\dot{v}_0 = \frac{(m - \Delta m)\,\dot{v}_1 + \Delta m \dot{v}_2}{m}, \tag{2}$$

where $\dot{v}_1$ and $\dot{v}_2$ are the velocities of the two masses immediately before the impact and $\dot{v}_0$ is the common velocity of the masses once they are moving together immediately after the impact. This condition on the collision might be achieved practically if a rapid clamping mechanism is used to attach the secondary mass to the primary mass.

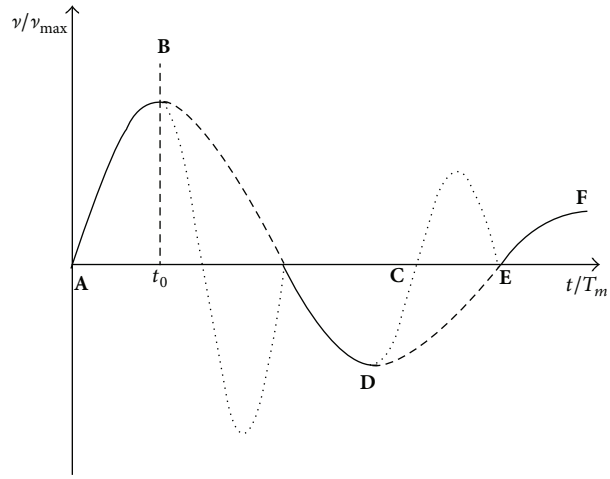

Figure 4: Response of the main mass $m - \Delta m$ before the stiffness reduction (–) and after the reduction (--). The dotted line represents the response of the secondary system when disconnected. Response is normalized to the maximum value, and time is normalized considering the mean period $T_m = (T_{\text{on}} + T_{\text{off}})/2$.

When the systems are attached, the equation of motion is as given by equation

$$m\ddot{\nu} + k_{\text{effective}}\nu = 0, \tag{3}$$

where m is the total mass and $k_{\text{effective}}$ is the effective total stiffness in the system. Following the control logic described by (1), when the displacement of the mass is maximum the stiffness is switched to its low value. At this point, the primary and secondary systems will oscillate independently and their equations of motion are

$$\begin{aligned}(m - \Delta m)\,\ddot{\nu}_1 + (k - \Delta k)\,\nu_1 &= 0,\\ \Delta m\ddot{\nu}_2 + \Delta k\nu_2 &= 0.\end{aligned} \tag{4}$$

The point at which the spring is disconnected is shown in Figure 4 as point B at time $t = t_0$.

Figure 4 also shows a general time-displacement response for the main mass $m - \Delta m$ until the stiffness recovery point. The system oscillates with a new natural frequency resulting from the effective stiffness and mass change until point C. The second mass is allowed to oscillate independently in a way that they do not collide or come together until a specified point in the cycle of vibration, which is marked as C in Figure 4 of the primary mass $m - \Delta m$. This process will repeat again from point D where the systems will be disconnected and eventually recombined at point E.

4. Energy Dissipation in the Compound Model

To obtain an expression for the energy dissipated during the impact, it is necessary to consider the exact values of velocity for each mass at the moment of contact. Considering the control law, the main mass $m - \Delta m$ is assumed to be passing through the static equilibrium position at the moment of contact or recovery, and the solution for the displacement of each mass can be found provided that the initial conditions are those from the stiffness reduction point B in Figure 4, that is, maximum displacement and zero velocity:

$$\begin{aligned}\nu_1 &= \nu_{\max}\cos\omega_p\left(t - t_0\right),\\ \nu_2 &= \nu_{\max}\cos\omega_s\left(t - t_0\right).\end{aligned} \tag{5}$$

The corresponding velocities are given by

$$\begin{aligned}\dot{\nu}_1 &= -\omega_p\nu_{\max}\sin\omega_p\left(t - t_0\right),\\ \dot{\nu}_2 &= -\omega_s\nu_{\max}\sin\omega_s\left(t - t_0\right).\end{aligned} \tag{6}$$

The natural frequencies for the disconnected single degree-of-freedom systems ω_p and ω_s (primary and secondary systems) are defined as

$$\begin{aligned}\omega_p &= \sqrt{\frac{k - \Delta k}{m - \Delta m}},\\ \omega_s &= \sqrt{\frac{\Delta k}{\Delta m}}.\end{aligned} \tag{7}$$

The time t_0 is the time it takes for both masses to oscillate for the first quarter of the cycle and it can be expressed as

$$t_0 = \frac{\pi}{2\omega_n}, \tag{8}$$

where ω_n is the natural frequency of the compound system when the masses are connected and is given by $\omega_n = \sqrt{k/m}$. At the moment of contact between the masses (marked as C in Figure 4), $t - t_0 = \pi/2\omega_p$ and the corresponding displacements and velocities of each mass can now be rewritten as

$$\nu_1 = 0, \tag{9}$$

$$\nu_2 = \nu_{\max}\cos\left(\frac{\pi\omega_s}{2\omega_p}\right), \tag{10}$$

$$\dot{\nu}_1 = -\omega_p\nu_{\max}, \tag{11}$$

$$\dot{\nu}_2 = -\omega_s\nu_{\max}\sin\left(\frac{\pi\omega_s}{2\omega_p}\right). \tag{12}$$

As stated by the control law the secondary mass needs to be at its static equilibrium point since its velocity is a maximum and this will increase the energy dissipation. It can be seen from (10) that this condition is possible only when the frequency ratio ω_s/ω_p takes odd integer values; that is, $\omega_s/\omega_p = 1, 3, 5, 7, \ldots$. The subsequent results are calculated using this condition. Thus, it is useful at this point to introduce the frequency ratio $\Omega = \omega_s/\omega_p$, the frequency ratio for the disconnected systems. It is now possible to calculate the energy lost during each impact. The kinetic energy after the impact is given by

$$T_0 = \frac{1}{2}m\dot{\nu}_0^2, \tag{13}$$

where $\dot{v}_0$ is the common velocity after the masses collide as given by (2). The initial total potential energy of the system is $(1/2)kv_{\max}^2 = (1/2)m\dot{v}_{\max}^2$, where $v_{\max}$ is the maximum peak displacement of the main system just before the secondary system is disconnected, and there is no energy lost until the point of zero displacement for the primary mass $m - \Delta m$ when the impact occurs. At this point, the energy dissipated during the impact is

$$E_d = \frac{1}{2}kv_{\max}^2 - \frac{1}{2}m\dot{v}_0^2. \tag{14}$$

Hence the corresponding percentage of energy dissipated can be expressed as a percentage of the energy in the system before the impact:

$$\%E_d = \left(1 - \frac{m\dot{v}_0^2}{kv_{\max}^2}\right) \times 100. \tag{15}$$

Combining (2), (14), and (15) the common velocity after the impact can be written as

$$\dot{v}_0 = \frac{v_{\max}}{m} \times \left[(m - \Delta m)\,\omega_p + \Delta m\omega_s \sin\left(\frac{\pi\omega_s}{2\omega_p}\right)\right]. \tag{16}$$

Equations (15) and (16) can be combined to give the percentage of energy dissipated as

$$\%E_d = \left[1 - \frac{1}{km} \times \left[(m - \Delta m)\,\omega_p + \Delta m\omega_p \sin\left(\frac{\pi\omega_s}{2\omega_p}\right)\right]^2\right] \times 100. \tag{17}$$

Equation (17) can be written in a nondimensional form by using the parameters $\sigma = \Delta k/k$, the stiffness reduction ratio, and the frequency ratio $\Omega = \omega_s/\omega_p$, the frequency ratio, to give

$$\%E_d = \left[1 - \frac{\sigma}{1 + \Omega^2\left((1/\sigma) - 1\right)} \times \left[\left(\frac{1}{\sigma} - 1\right)\Omega + \sin\left(\frac{\pi}{2}\Omega\right)\right]^2\right] \times 100. \tag{18}$$

The mass ratio $\mu = \Delta m/m$ as defined previously is used again. To guarantee that the masses coincide at the static equilibrium displacement position at the time required, μ and σ must have values that satisfy $\Omega = \omega_s/\omega_p = 1, 3, 5, \ldots$, that is, odd integers. However, in the case of $\mu = \sigma$, which gives $\Omega = 1$, the amount of energy dissipated is zero. This is because the velocity of the secondary mass is equal in magnitude and phase to the velocity of the main mass when they collide; that is, the relative approach velocity is zero. There is no change in the velocity of the masses before and after the impact, so there is no energy lost during the contact.

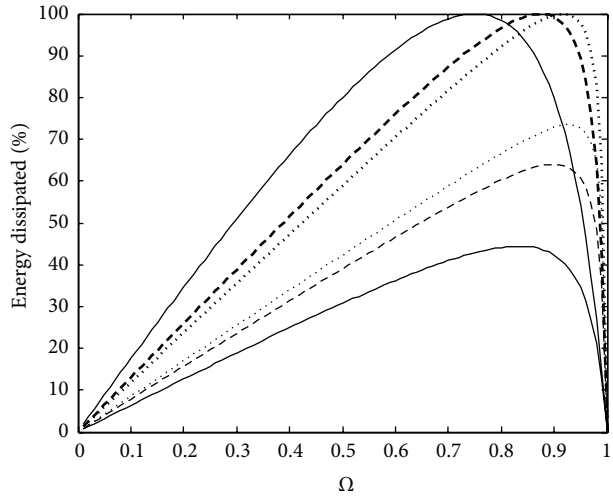

Figure 5: Percentage of energy dissipated at the first reconnection as a function of the stiffness reduction ratio σ for different values of the secondary to primary systems frequency ratio Ω (—$\Omega = 3$; - - - $\Omega = 7$; $\cdots$ $\Omega = 11$; —$\Omega = 5$; – – $\Omega = 9$; - - - $\Omega = 13$).

In order to assure maximum energy dissipation during the impact the common velocity of the masses after the contact must be as small as possible; that is, the kinetic energy is minimized. Since the velocity of the mass $m - \Delta m$ is always a maximum just before the impact, the velocity of Δm should preferably be a maximum and have opposite sign at the point of impact. This is not necessarily true for all the odd integer values of Ω as the energy dissipated is considerably higher when $\Omega = 3, 7, 11, \ldots$. On the other hand, when $\Omega = 5, 9, 13, \ldots$ the energy dissipated is smaller. It is possible to maximize the energy dissipation when $\Omega = 3, 7, 11, \ldots$ because the velocity of the masses is out of phase at the moment of impact. However, when $\Omega = 5, 9, 13, \ldots$ the velocities, although different in magnitude, have the same phase; therefore the energy dissipation is considerably less compared with the previous case. This fact can be seen clearly in Figure 5, which shows the energy dissipation as a function of the stiffness ratio, for the values of Ω mentioned above.

Although no damping is included in the modeling of the system, it is useful to obtain an equivalent viscous damping ratio in order to quantify the energy dissipated in the model and compare with the well-known MKC system. A plot of the equivalent viscous damping ratio as a function of the stiffness reduction factor σ is presented for several values of Ω in Figure 6. Although the decrement of peak amplitudes is not logarithmic, it can be considered as such for simplicity and comparison to the viscously damped system. As a result, (18) can be used to calculate the amplitude ratio of consecutive peaks and then the logarithmic decrement as $\delta = \ln(v_1/v_2)$ and hence the equivalent damping ratio is estimated using the well-known equation $\zeta = \delta/\sqrt{4\pi^2 + \delta^2}$; this plot further confirms the energy dissipation behaviour. The equivalent viscous damping ratio was obtained numerically by obtaining the peak displacements for the impacting model, using a fourth order Runge-Kutta routine, and then considering the

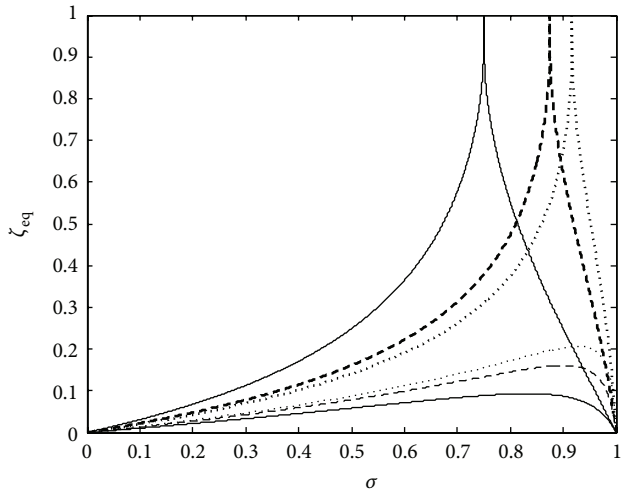

Figure 6: Equivalent damping ratio ζ_{eq} as a function of the stiffness reduction ratio σ for different values of the secondary to primary system frequency ratio Ω (—$\Omega = 3$; - - - $\Omega = 7$; $\cdots$ $\Omega = 11$; —$\Omega = 5$; – – $\Omega = 9$; - - - $\Omega = 13$).

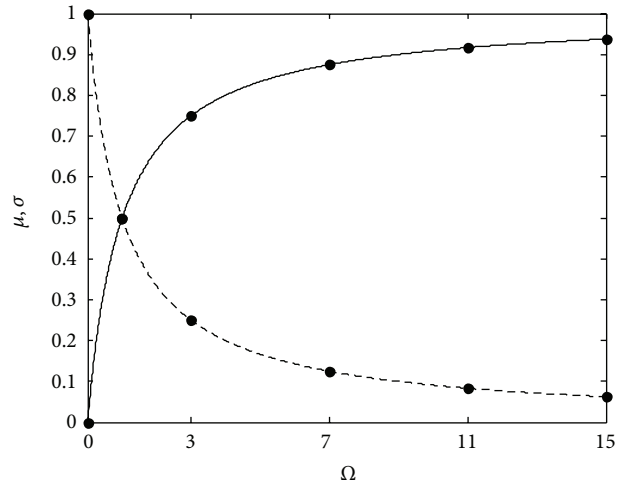

Figure 7: Values of the stiffness reduction ratio σ and mass ratio μ corresponding to different values of secondary to primary system frequency ratio Ω which give maximum energy dissipation in the impacting model (— σ; - - - μ).

decay rate. The calculations were made for $\Omega = 3, 5, 7, 9, 11$, and 13 as a function of the stiffness reduction factor.

When $\Omega = 3, 7, 11, \ldots$ there is an optimum combination of μ and σ for each value of Ω, which dissipates all the energy during the first impact. As a result both masses return to rest immediately after the impact. This condition can be stated mathematically considering the total momentum after the impact is zero, as follows:

$$(m - \Delta m)\, x_{\max}\omega_p - \Delta m x_{\max}\omega_s = 0. \tag{19}$$

Noting that $\Omega = \omega_s/\omega_p$, (19) can be written as

$$\frac{m - \Delta m}{\Delta m} = \Omega. \tag{20}$$

Thus, for $\Omega = 3, 7, 11, \ldots$ the relationship between the optimum mass ratio and the frequency ratio is given by

$$\mu = \frac{1}{\Omega + 1}. \tag{21}$$

Using (7) the frequency ratio can also be expressed as $\Omega = \sqrt{(1-\mu)\sigma/(1-\sigma)\mu}$. As a result, the relationship between the stiffness ratio and the frequency ratio can be calculated as

$$\sigma = \frac{\Omega}{\Omega + 1}. \tag{22}$$

The values of μ and σ calculated using (21) and (22) represent the peaks observed in Figure 6 for $\Omega = 3, 7, 11, \ldots$. These peaks tend to indicate an equivalent damping ratio of 1, which is true considering the definition of critical damping as the system no longer possesses oscillation. Hence, it is possible to maximize the energy dissipation for these situations. This can be further validated by obtaining the derivative of (18), which can be used to obtain the maximum value of energy dissipation for particular values of Ω. However, as Ω increases, the stiffness reduction required also increases, which could be difficult to achieve in practice. The corresponding values of μ and σ for discrete values of Ω which give maximum energy dissipation are shown in Figure 7, where it is clearly seen that higher stiffness reduction is needed as Ω increases.

In general the stiffness and mass ratios can be related using the following equation:

$$\mu = \frac{1}{1 + \Omega^2\left((1/\sigma) - 1\right)}. \tag{23}$$

As an example, consider the plot shown in Figure 8(a) which depicts a time history showing the displacement, velocity, and acceleration responses for the impacting model (bold line) where $\sigma = 0.5$ and $\mu = 0.1$. The sudden changes in velocity are due to the impact between the masses after every half cycle. This combination will give $\Omega = 3$ but is not optimized for the case of maximum energy dissipation. The optimum situation when the energy dissipated is maximized, that is, $\mu = 0.25$ and $\sigma = 0.75$, is presented in Figure 8(b).

Figure 9(a) shows the secondary system response (dashed line) during the times it remains disconnected and oscillates independently, showing that both masses coincide at the same point during the impact. Figure 9(b) shows the kinetic, potential, and total energy for the system. This plot shows the sum of the energies in the primary and the secondary systems. Both Figures 9(a) and 9(b) are for values of $\sigma = 0.5$ and $\mu = 0.1$. The results corresponding to the optimum situation occurring when $\mu = 0.25$ and $\sigma = 0.75$ are shown in Figure 10, where it is clearly seen that the masses are at rest immediately after the first impact.

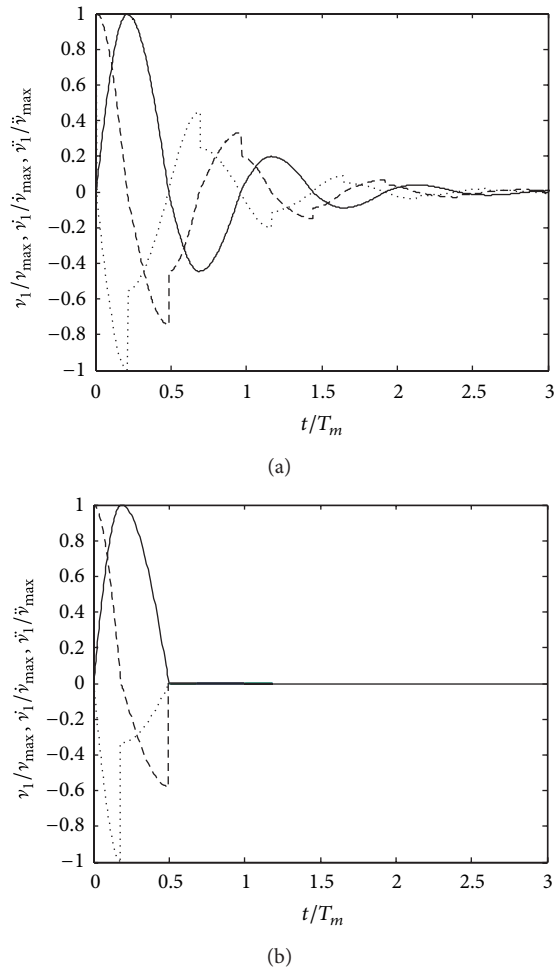

Figure 8: Time response for the impacting model. The time is normalised with respect to the mean period T_m. (a) $\sigma = 0.5$ and $\mu = 0.1$, (b) $\sigma = 0.75$ and $\mu = 0.25$. The frequency ratio between secondary and primary system is $\Omega = 3$ (— displacement; - - - - velocity; ⋯ acceleration).

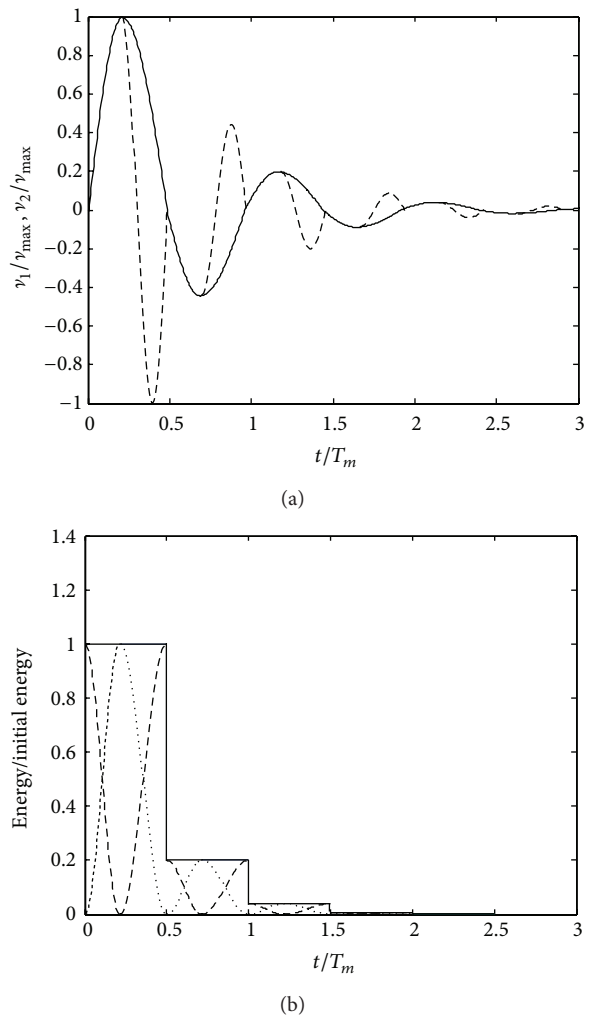

Figure 9: (a) Displacement response for both the main (—) and the secondary system (- - -). (b) Energy levels in the system (— total energy; - - - kinetic energy; ⋯ potential energy). Time is normalised with respect to the mean period T_m. For this example the stiffness reduction ratio is $\sigma = 0.5$ and the mass ratio $\mu = 0.1$, giving a secondary to primary system frequency ratio $\Omega = 3$.

5. Comparison with the Massless Secondary System

In order to establish a relationship between this impacting model and the basic model considered in [7] one can consider the behaviour of the impacting model when the secondary mass tends to zero. The maximum energy in the basic switchable stiffness model can be written in terms of the potential energy as $(1/2)k\nu_{max}^2$. The percentage of energy dissipated after the first stiffness reduction (half a cycle) can be expressed as

$$\%E_d = \frac{(1/2)\,k\nu_{max}^2 - (1/2)\,k\nu_{min}^2}{(1/2)\,k\nu_{max}^2} \times 100, \tag{24}$$

where ν_{min} is the subsequent negative peak displacement (marked as D in Figure 2) and it is related to ν_{max} by $\nu_{min} = \nu_{max}\sqrt{1-\sigma}$. It is important to note that there are two stiffness reductions for the basic model, as there are in general apart from the optimum cases two impacts in the impacting model each cycle. Hence, (24) reduces to

$$\%E_d = \sigma \times 100. \tag{25}$$

Equation (25), which gives the energy dissipation as a result of the first stiffness reduction in the cycle, coincides with the energy dissipation in the impacting model during the first impact, assuming a very small fixed value of the secondary mass; that is, $\mu \approx 0$. This can be easily shown if

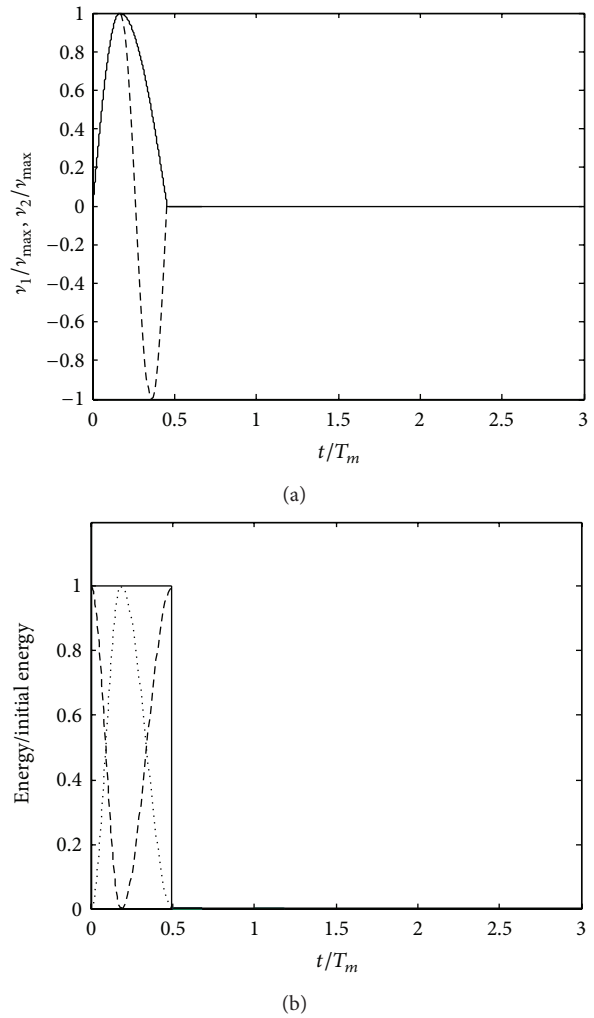

FIGURE 10: (a) Displacement response for both the main (—) and the secondary system (- - -). (b) Energy levels in the system. Time is normalised with respect to the mean period T_m. For this example the stiffness reduction ratio is $\sigma = 0.75$ and the mass ratio $\mu = 0.25$, giving a secondary to primary system frequency ratio $\Omega = 3$ and maximum energy dissipation (— total energy; - - - kinetic energy; ⋯ potential energy).

(18) is expressed in terms of the mass ratio μ and the stiffness ratio reduction σ giving

$$\%E_d = \left[1 - \left[\sqrt{1-\sigma}\sqrt{1-\mu} + \sqrt{\mu\sigma}\sin\left(\frac{\pi}{2}\sqrt{\frac{(1-\mu)\sigma}{(1-\sigma)\mu}}\right)\right]^2\right] \times 100. \tag{26}$$

By setting $\mu = 0$ in (26) and simplifying the resulting expression equals (25) thus showing how the compound model reduces to the simple model when the secondary mass is negligible.

6. Effect of Damping and Equivalent Viscous Damping Ratio

The objective of the switchable stiffness strategy is to reduce or minimise the residual vibration in lightly damped systems after a shock has been applied to a system. So far, the impacting model has been analyzed, without taking into account any damping. In this section, a brief investigation is conducted as to whether the impact strategy would have any benefit if applied to a system that already has some damping present. This is important because all real systems inherently have some form of damping.

Figure 11 represents a viscously damped single degree-of-freedom system with two parallel springs one of which can be disconnected using the control law given by (1). When disconnected there are two independent mass-spring-damper systems. When both systems are attached an equivalent damping constant is calculated from the constants c_p and c_s corresponding to the damping constants of the primary and secondary systems, respectively. Additionally, viscous damping ratios for the primary and secondary systems are introduced as ζ_p and ζ_s, respectively.

The displacement response for the primary and secondary masses from the maximum displacement point (i.e., point B in Figure 4, but now considering damping) is given, respectively, by

$$v_1 = 0, \tag{27}$$

$$v_2 = v_{max}\, e^{-\zeta_s\omega_s(t-t_0)}\cos\left(\omega_s\sqrt{1-\zeta_s^2}\,(t-t_0)\right). \tag{28}$$

The time t_0 is given by (8) as in the undamped case. The percentage of the energy dissipated can be obtained calculating the common velocity of the masses $\dot{v}_0$ after they impact and oscillate together, as expressed by (2). Using the derivatives of (27) and (28) and then combining them into (2) give the common velocity after the impact. As a result the percentage of energy dissipated during the impact in the damped impacting model can be expressed as

$$\%E_d = \left[1 - \frac{\sigma}{1+\Omega_d^2\left((1/\sigma)-1\right)} \times \left[e^{-\pi\zeta_p/2\sqrt{1-\zeta_s^2}}\left(\frac{1}{\sigma}-1\right)\Omega_d\sqrt{1-\zeta_p^2} + e^{\pi\zeta_s\Omega_d/2\sqrt{1-\zeta_p^2}} \times \left[\zeta_s\cos\left(\frac{\pi}{2}\Omega_d\right) + \sqrt{1-\zeta_s^2}\sin\left(\frac{\pi}{2}\Omega_d\right)\right]\right]^2\right] \times 100, \tag{29}$$

where the frequency ratio Ω has been replaced by the damped frequency ratio, since the model is now damped. This ratio is defined as

$$\Omega_d = \frac{\omega_s\sqrt{1-\zeta_s^2}}{\omega_p\sqrt{1-\zeta_p^2}}. \tag{30}$$

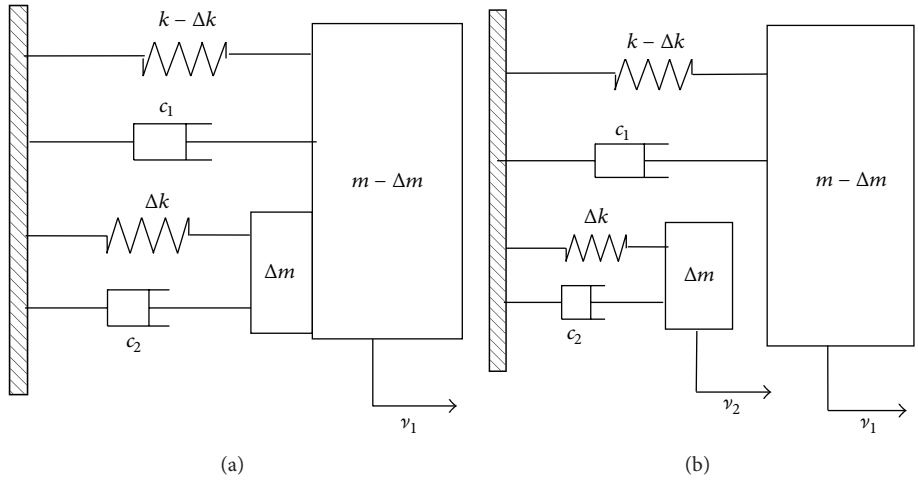

Figure 11: On-off stiffness model with viscous damping model considering a secondary spring with mass: (a) the systems are rigidly attached; (b) the secondary mass is disconnected and oscillates independently of the main mass.

As described in the previous section, one wants the frequency ratio to have values $\Omega_d = 3, 7, 11, \ldots$ in order to maximize energy dissipation and ensure the systems can recombine at the required times. Thus, the physical properties of the system must be tuned to keep the required frequency ratio.

In order to evaluate the performance of this system a key parameter to compare is the equivalent damping ratio of the system. It is difficult to obtain an analytical expression for the equivalent damping, since the effective damping will comprise the effect of the viscous damping present in the system and the energy dissipated by the stiffness reduction. Additionally, the damping ratio of the system will change over time as a result of the stiffness and mass variations. However, it is relatively straightforward to estimate the effective damping by using (26) to calculate the energy dissipation and then find the consecutive peaks used to obtain the equivalent logarithmic decrement. For the numerical results in this section, the damping constants c_p and c_s are selected so that the damping ratio for both systems is the same; that is, $\zeta_1 = \zeta_2$. The effective damping ratio is shown in Figure 12 for several values of the initial damping ratio in the system for the on period, as a function of the stiffness reduction factor, considering $\Omega_d = 3$.

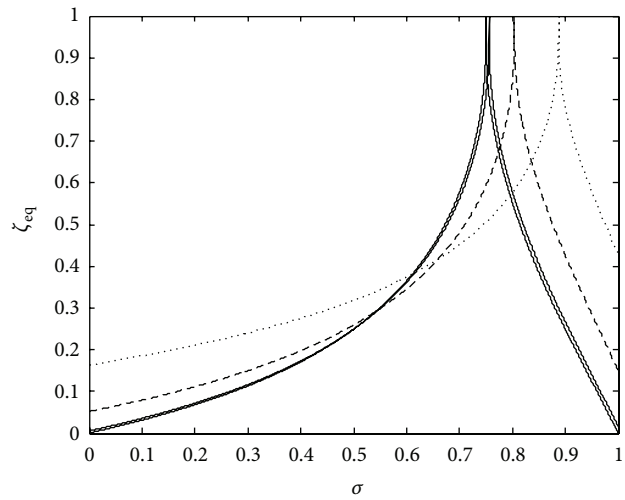

Figure 12: Equivalent damping ratio ζ_{eq} for the impacting system considering viscous damping in both primary and secondary systems, considering the same damping ratio in both systems, so $\zeta = \zeta_1 = \zeta_2$. The frequency ratio is $\Omega_d = 3$ (—$\zeta = 0$; —$\zeta = 0.01$; – – $\zeta = 0.1$; - - -$\zeta = 0.3$).

This condition will shift the optimum values of μ and σ, but the frequency ratio Ω_d will remain the same. The equivalent damping ratio will be enhanced as the viscous damping in the system increases. However, the main conclusion from this figure is that there is no significant change if the system is lightly damped, for instance, when the fraction of critical damping is less than 5%. There is a limit on how much equivalent damping can be obtained depending on the amount of physical damping present in the system. It is important to remember that the strategy is suitable for low damping systems, where the addition of any other form of damping is not straightforward. Otherwise, if the system is already highly damped it can be more convenient from a practical point of view not to use a semiactive strategy but simply to add another form of passive damping. Finally, Figure 13 compares two situations; the first one depicted by the continuous line represents the equivalent damping ratio when $\Omega_d = 3$ and a damping ratio of 0.01. On the other hand, the dotted line shows the equivalent damping for the basic model as explained in [9], considering a damping ratio of 0.01. As a result, it can be seen that the impacting model presents a practical limiting value of stiffness reduction where the energy dissipation is optimized, rather than the physically unrealisable value of 100% stiffness reduction of the basic model when energy dissipation is maximized. Moreover, it appears that the impacting model at low values of stiffness reduction always exceeds the performance of the basic on-off stiffness model in terms of energy dissipation. If the

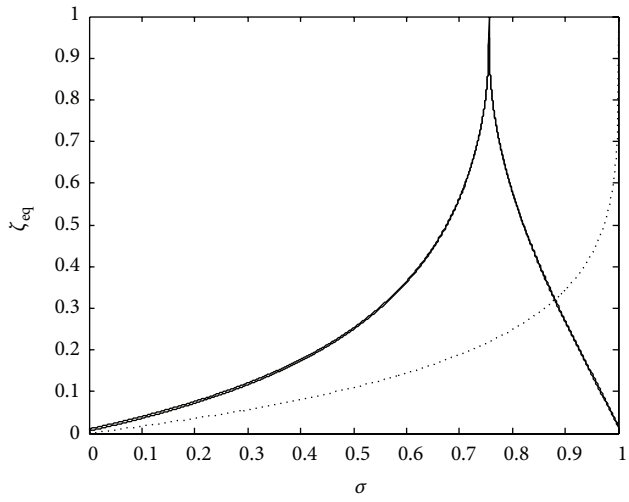

Figure 13: Equivalent damping ratio comparison between an impacting model, considering a frequency ratio of $\Omega = 3$ (—), and the same model when the secondary mass approaches zero ($\cdots$). The viscous damping ratio considered for both models is the same and is equal to 1%.

parameters of the model are adequately chosen, the energy lost by the inelastic impacts is higher than the energy lost in the simple model by the disconnecting spring.

7. Conclusions

An alternative modelling approach has been proposed, in order to investigate the energy dissipation in a switchable stiffness system and to provide a valid mathematical and physical model. This approach involved a secondary spring with a small mass and considers the impact between this mass and the main mass at the moment of stiffness recovery. The energy is solely dissipated due to this inelastic impact. There is a trade-off between the mass and stiffness ratios; high energy dissipation can be achieved for certain combinations of these parameters which are physically allowed. It was found that as the secondary mass is reduced to zero, this system effectively reduces to the energy dissipation characteristics for the basic on-off model.

Furthermore, the inclusion of viscous damping was studied in both the basic and the impacting systems. The main conclusion obtained being that when the system is lightly damped the performance is not affected. However, highly damped systems experience a drawback in vibration suppression, and the effective damping ratio could become lower than that for the viscous damping ratio present for the passive linear original system. This supports the hypothesis that the strategy is only suitable and beneficial to improve residual vibration control in lightly damped systems.

Conflict of Interests

The authors declare that there is no conflict of interests regarding the publication of this paper.

Acknowledgments

The authors would like to acknowledge the Mexican Council for Science and Technology CONACyT for the financial support and the Universidad Autónoma de Nuevo León, UANL.

References

[1] C. M. Harris and C. E. Crede, *Shock and Vibration Handbook*, McGraw-Hill, New York, NY, USA, 1996.

[2] R. S. Ayre, *Engineering Vibrations*, McGraw-Hill, New York, NY, USA, 1958.

[3] J. C. Snowdon, *Vibration and Shock in Damped Mechanical Systems*, Wiley and Sons, New York, NY, USA, 1968.

[4] R. L. Eshleman and P. Rao, "Response of mechanical shock isolation elements to high rate input loading," *Shock and Vibration Bulletin, Shock and Vibration Information Center*, vol. 40, no. 5, pp. 217–234, 1969.

[5] D. V. Balandin, N. N. Bolotnik, and W. D. Pilkey, "Review: optimal shock and vibration isolation," *Shock and Vibration*, vol. 5, no. 2, pp. 73–87, 1998.

[6] D. V. Balandin, N. N. Bolotnik, and W. D. Pilkey, "Pre-acting control for shock and impact isolation systems," *Shock and Vibration*, vol. 12, no. 1, pp. 49–65, 2005.

[7] T. P. Waters, Y. Hyun, and M. J. Brennan, "The effect of dual-rate suspension damping on vehicle response to transient road inputs," *Journal of Vibration and Acoustics, Transactions of the ASME*, vol. 131, no. 1, 2009.

[8] D. F. Ledezma, N. S. Ferguson, and M. J. Brenan, "Shock performance of different semiactive damping strategies," *Journal of Applied Research and Technology*, vol. 8, no. 2, pp. 249–259, 2010.

[9] D. F. Ledezma-Ramirez, N. S. Ferguson, and M. J. Brennan, "Shock isolation using an isolator with switchable stiffness," *Journal of Sound and Vibration*, vol. 330, no. 5, pp. 868–882, 2011.

[10] D. F. Ledezma-Ramirez, N. S. Ferguson, and M. J. Brennan, "An experimental switchable stiffness device for shock isolation," *Journal of Sound and Vibration*, vol. 331, no. 23, pp. 4987–5001, 2012.

[11] J. Onoda, T. Endo, H. Tamaoki, and N. Watanabe, "Vibration suppression by variable-stiffness members," *AIAA journal*, vol. 29, no. 6, pp. 977–983, 1991.

[12] D. K. Anand and P. F. Cunniff, *Engineering Mechanics: Dynamics*, Houghton Mifflin Company, Boston, Mass, USA, 1973.